# Photophysical Studies on the Mono- and Dichromophoric Hemicyanine Dyes III. Ultrafast Fluorescence Up-conversion in Methanol: Twisting Intramolecular Charge Transfer and "Two-State Three-Mode" Model

**Yanyi Huang, Tianrong Cheng, Fuyou Li, and Chun-Hui Huang***

*State Key Laboratory of Rare Earth Materials Chemistry and Applications, and College of Chemistry and Molecular Engineering, Peking University, Beijing 10871, China*

**Shufeng Wang, Wentao Huang, and Qihuang Gong**

*State Key Laboratory of Mesoscopic Physics, and College of Physics, Peking University, Beijing 100871, China*

*Received: April 3, 2002; In Final Form: July 13, 2002*

A series of hemicyanine dyes, including monomer ([(*E*)-*N*-methyl-4-(2-(4-*N*,*N*-dimethyl phenyl) ethenyl) pyridinium] iodide; M) and dimers (1,*n*-Bis [(*E*)- 4-(2-(4-*N*,*N*-dimethyl phenyl) ethenyl) pyridinyl]-alkane dibromide; $n = 3$, alkane = propane, B3; $n = 5$, alkane = pentane, B5; $n = 12$, alkane = dodecane, B12), are synthesized and their ultrafast fluorescence up-conversion behaviors are studied. The fluorescence decay curves of these dyes can be well fitted by the sum of several exponential decays in the shorter wavelengths and by the sum of the exponential rise(s) with decay(s) in the longer wavelengths. The fact that the values of longest lifetime component at longer wavelengths tend to be a constant proves the existence of a "sink" region on the potential energy surface of excited state. This sink region is around the TICT state, by which the nonradiative transition dominates the deactive decay paths of excited state. The time dependent Stokes shift function analysis of these four dye molecules in methanol indicates that the B5's unique "solvation" behavior is different from others. This difference is contributed by the increased difficulty of the TICT formation of B5 originated from its folded conformation. The time dependent Stokes shifts of M, B3, and B12 are due to not only solvation dynamics but also TICT formation. Detailed analysis is presented in the frame of a "two-state three-mode" model.

## 1. Introduction

Hemicyanine and its derivatives are important for their potential applications in the field of molecular electronics,[1] lasers,[2] and biology.[3,4] The unique photophysical properties of hemicyanine chromophore strongly correlate to its chemical structure. With a strong electronic pushing group (amine) on one end of the chromophore and a strong electronic withdrawing group (pyridium) on the other end, hemicyanine has extremely large dipole moments in the ground state. A charge transfer, i.e., the positive charge transfers from the pyridium moiety to the amine group, occurs when excited to the singlet excited state.[5] This great change in the dipole moment between ground state and excited state is the reason for the excellent performance of the second harmonic generation (SHG) of hemicyanine chromophore.[5−7] Our investigation in the relationship between the chemical structure and the properties shows that the change of electronic structure with excitation also plays an important role in the photoelectro conversion (PEC) ability.[8−13] Furthermore, we have found that some dimers and multichromophoric derivatives can remarkably enhance the SHG and PEC abilities.[11−13] To date, the nature of this enhancement by joining the chromophores together has not been thoroughly understood.

In recent years, there have been quite a few reports on the synthesis and physical properties of the dimers.[14−21] Usually, the dimerization of chromophores can cause the obvious change in such steady-state spectra as absorption and fluorescence. These changes, especially the peak-shifts of spectra, can be easily interpreted as the formation of intramolecular aggregates or the interchromophore delocalization. However, no such kind of interaction is observed in our research on the dimers of hemicyanine with methylene groups as linkages through the steady-state spectra.[22,23]

The significant developments during the past two decades with regard to laser technique and precise controlling make the femtosecond time-resolved spectroscopic measurement possible. Ultrafast fluorescence up-conversion is a powerful technique for measuring the emission decay process with femtosecond resolution and for determining the ultrafast evolution path of excited-state wave packet. There are many reports on the solvation dynamics by using femtosecond fluorescence up-conversion and on the successes in achieving parameters of solvation response.[24] Actually, the relaxations that occur in solution after the excitation of the electronic state of a solute include both the configurational rearrangement of the solvent molecules and the evolution of the excited state of the solute molecule to an equilibrium state. Moreover, these two processes are strongly coupled.[25,26] The detailed process of the relaxation of solute molecule consist of the stretching and torsion motions of cyanine chromophores, and recent quantum chemical calculations show that there is strong interplay between these two modes for short length cyanines.[27] The experimental studies on the common polar solvent such as water, methanol, and acetonitrile are very important to explore details of chemical

* To whom the correspondence should be addressed. E-mail: hch@chem.pku.edu.cn.

10.1021/jp0208788 CCC: $22.00 
Published on Web 09/07/2002

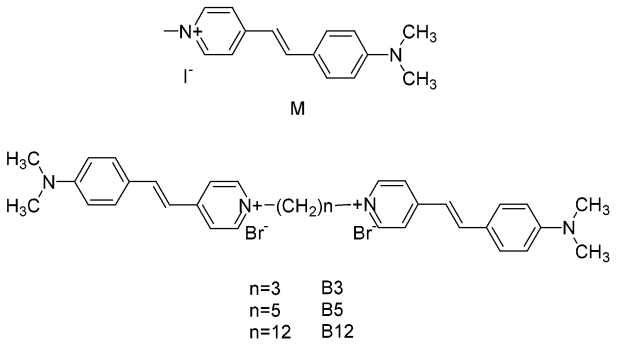


**Figure 1.** Chemical structures of dyes.

reactions in solutions, and results show that their solvation response correlation function can be expressed as the sum of an ultrafast ($\sim 10^2$ fs) Gaussian component which comes from the collisionless rotational motions within the solvent cage, and several exponential components which are due to the diffusive (rotational diffusion) motions of the solvent molecules.[28−30] This result has been further confirmed by theoretical calculations[31] and other experimental methods.[32] To our knowledge, there are few reports on the ultrafast spectroscopic research of dimers.

We present here the study of the ultrafast fluorescence up-conversion of a series of hemicyanine dyes (Figure 1) which contain one monomer (M) and three dimers (B3, B5, and B12) with different lengths of alkyl linkages. By considering the interplay of solvation, stretching and torsional motions, a "two-state three-mode" model is applied to explain the experimental results. After reconstructing the emissive spectra, the time dependent Stokes shift functions (TDSSF) of these four dyes are obtained by curve fitting via a function expressed by combining one ultrafast Gaussian component and two exponential decays. By comparing our results with the results of DCM[29] and Coumarin,[30] the TICT state formation also contributes to the TDSS and couples with other relaxation processes in M, B3, and B12, whereas for B5, the TICT contribution is not distinct in the TDSSF. Taking the difference of conformation into account, the folded shape of B5, which can influence the twisting motion of the chromophore, is the reason for the characteristic behavior in the TDSS.

## 2. Experimental Section

**2.1. Materials.** All dyes (Figure 1) are synthesized via the condensation reactions. The details of synthesis procedure will be published elsewhere.[22] The purities and chemical structures of our dyes have been tested by NMR and elements analysis. The solvent, methanol, is A. R. grade and purchased from Beijing Chemical Factory, China. It is purified by distilling before using.

**2.2. Steady-State Spectroscopy.** Absorption spectra are taken by a Shimadzu UV 3101 PC UV−vis−NIR spectrophotometer (Shimadzu, Japan), with pure solvent as reference. Fluorescence spectra are measured by a Hitachi F4500 fluorescence spectrophotometer (Hitachi, Japan).

**2.3. Femtosecond Fluorescence Up-Conversion Setup.** Fluorescence decays of hemicyanine monomer and dimers are measured by the femtosecond fluorescence up-conversion setup described in Figure 2. There are a CW Ar+ laser (Innova 415, Coherent, USA) pumps a Ti:sapphire laser (Mira 900F, Coherent, USA) producing the pulse at 830 nm with duration of 110 fs, at a repetition of 76 MHz. The output energy of the pulse is around 20 nJ/pulse. The second harmonic is generated by focusing the output pulses to a 1 mm thick BBO crystal. The fundamental frequency beam and the second harmonic beam are split by a dichromic mirror; the former one is used for gating pulses, and the latter is used for pumping (wavelength is 415 nm). The pumping light is focused onto a 1-mm thick quartz flowing sample cell. The dye solutions are circulated through this flowing cell by a peristaltic pump. The flowing rate is about 30 mL/min. The fluorescence was collected and a low-pass filter is used to remove the excitation light. The fluorescence goes through a polarizer, which is tuned to fit the magic angle to avoid the effects of rotational diffusion of the molecule. The up-conversion signal is generated by focusing the fluorescence beam together with the gating beam onto another 1 mm BBO crystal with type I phase matching conditions. This up-conversion signal is finally focused on the entrance slit of a monochromator and detected by means of a photomultiplier (Hamamatsu R585) connected to a photon counter (Hamamatsu C5410). The typical step size of the decay measurement is 6 fs. The instrumental response function is measured by the cross-correlation of the pumping and gating pulses.

**2.4. Computational Method.** Semiempirical quantum calculations are used to determine the energy surface of the excited state and ground state of hemicyanine with torsion through the dimethyl amino group (twisting the C−N bond) and through the aniline ring (twisting the C−C bond). The AM1 Hamilton

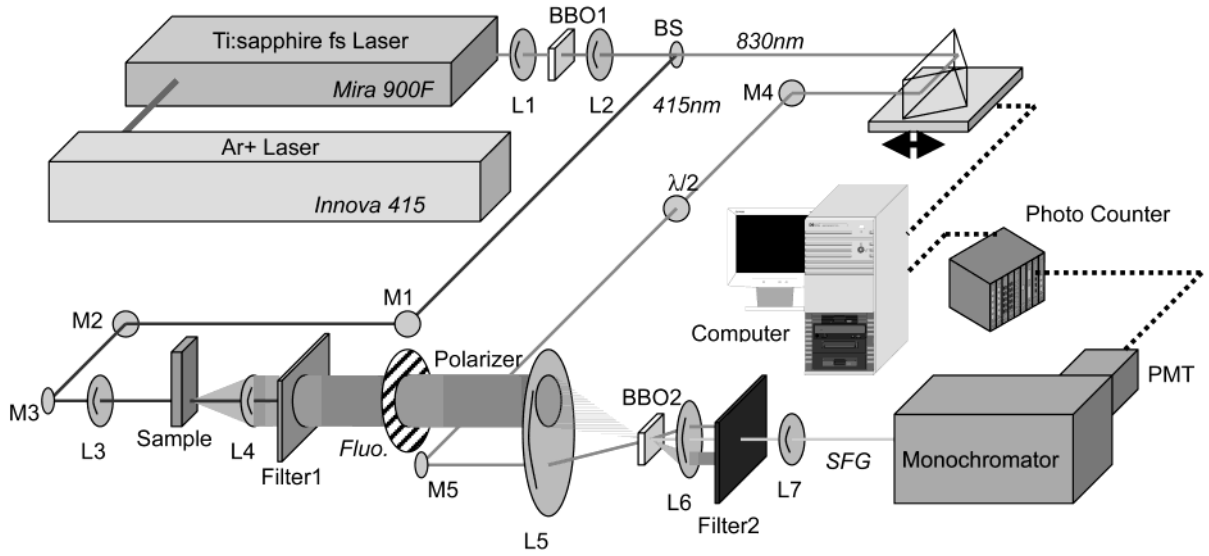


**Figure 2.** Femtosecond fluorescence up-conversion setup. L: lens; M: mirror.

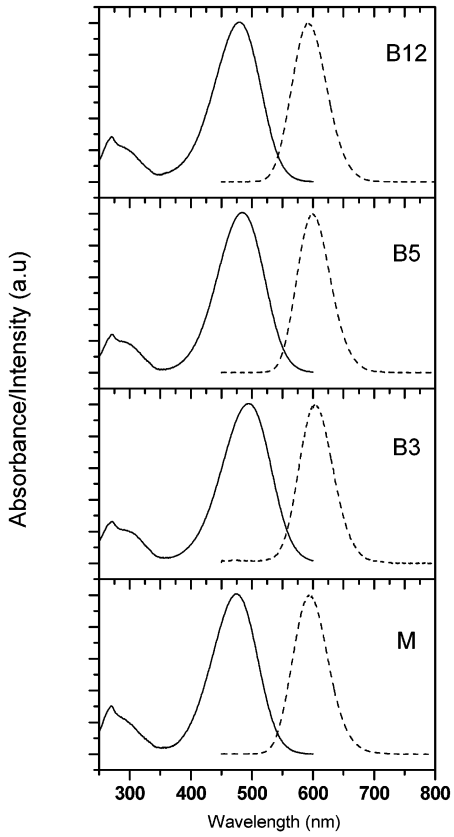


**Figure 3.** Steady-state absorption and fluorescence spectra of dyes. The excitation wavelength of fluorescence spectra is 415 nm.

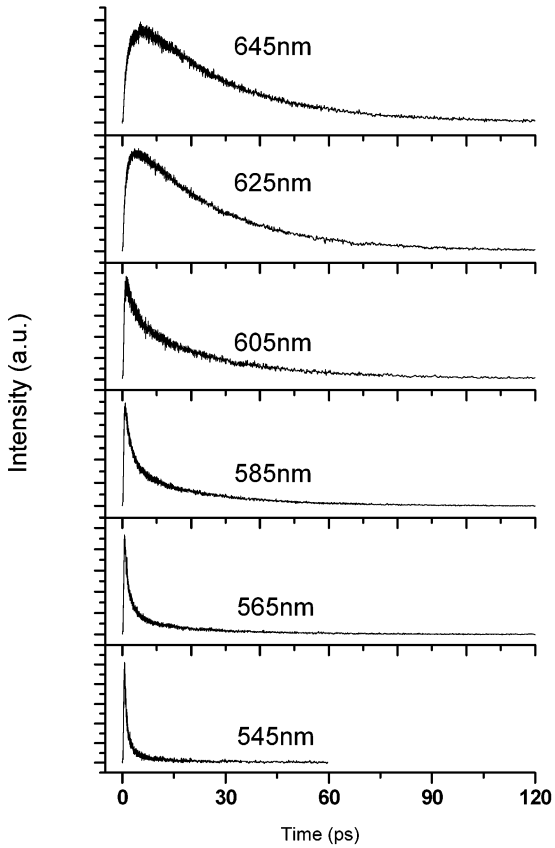


**Figure 4.** Representative fluorescence up-conversion decays of M in methanol at different detection wavelength.

is applied and MOPAC package is carried for calculations. Each of the conformations is optimized via the molecular mechanics method followed by the AM1 method with fixing the corresponding torsion angle.

## 3. Results and Discussion

**3.1. Steady State Spectroscopy.** The two chromophores in one dimer molecule are certainly correlated, and the action of one chromophore affects the other one. There are several reports on the intramolecular aggregate formation in dimers of other chromophores. The absorption spectra and fluorescence spectra of our four hemicyanine dyes in methanol have been shown as Figure 3. Their absorption spectra, as well as their fluorescence spectra are similar to each other among these four dyes. The absorption peak around 500 nm is due to the transition from $S_0$ to $S_1$ of the individual chromophore, and this transition will change the charge distribution of chromophore dramatically. There are several reports on the aggregate formation of the hemicyanine chromophore, and the results show that hemicyanine can form H-aggregate in some conditions, such as in LB films and in those nonpolar (or weak polar) solvents; the absorption of this H-aggregate is a strong band around 300 nm.[33] The peak around 500 nm is just slightly affected by the dimerization, and this slight difference can be assumed to result from the difference of the linkage groups (vide infra), indicating the weak interaction between the two chromophores in one dimer molecule. Furthermore, the concentration of the solution will not change the shapes and the peak positions of these dyes. To summarize, there is no evidence for the formation of either the "intramolecular aggregate" or the "intermolecular aggregate" here; that is, there is no strong exciton coupling interaction between either the two chromophores of one dimer molecule or the chromophores of different molecules in methanol solutions. This result corresponds with the recent studies of some dimers of similar chromophores reported by Thomas et al.[20] In that case, changing the temperature and the polarity of a solvent led to a conformational switch between a folded conformation and an unfolded one in a dimer.

The negative result of the formation of the aggregate of hemicyanine dimers in methanol does not mean that the properties of hemicyanine cannot be changed by dimerization. Our former report on the photoelectro conversion and the picosecond resolved fluorescence behavior in chloroform solution has shown the difference between the dimers and the monomer.[22,23] The difference between the dimers is the linkage moiety between two hemicyanine chromophores. B3 and B5 has relatively short-length linkages between two hemicyanine chromophores, and the distance between the two chromophores is in a magnitude of several Angstroms, whereas the linkage in B12 is relatively long (twelve methylene groups), and the distance between the two chromophores is much larger. Generally speaking, compared with B3 and B5, B12 shows more similarity to the monomer because the two chromophores in B12 are quite well separated from each other. B3 and B5 have only slight red-shifted absorption peaks compared with M and B12, indicating that the dimerization can really affect the delocalization of chromophore (although this effect is rather weak): a shorter distance may bring a higher possibility for "interchromophore delocalization", which is similar to the expanse of the conjugating degree of the chromophore and consequently red-shifts the absorption band.

**3.2. Femtosecond Fluorescence Up-Conversion Measurements.** Representative fluorescence up-conversion decays of M in methanol are shown in Figure 4 , and the wavelength values listed in the figure are those detecting wavelengths at which

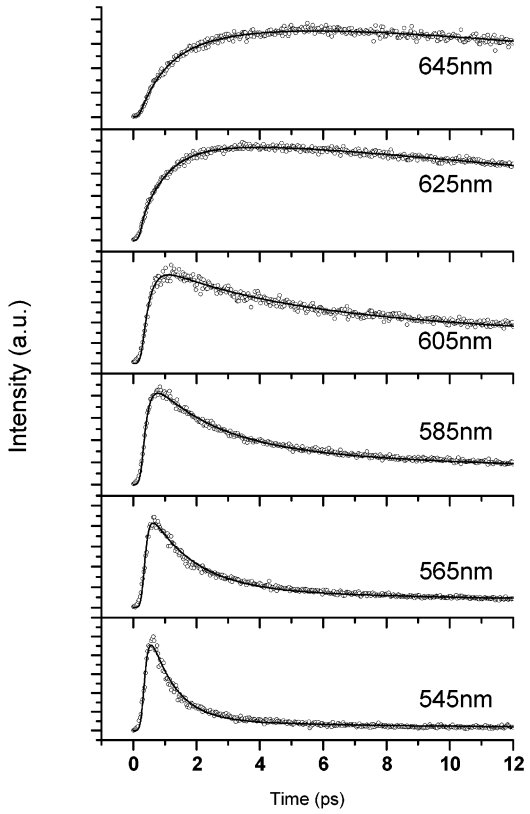


**Figure 5.** Initial several picoseconds of Figure 4.

the fluorescence signals are collected. The excitation light is the second harmonic generation of the fs Ti:sapphire laser, whose wavelength is located at 415 nm. This excitation wavelength is in the blue edge of the absorption band of these dyes, indicating that the Franck−Condon state will located in the high vibration level of the singlet excited state. The detailed illustrations of the initiative several picoseconds after the fs pumping laser excitation of those representative decays are shown in Figure 5. Obviously, the fluorescence decays are dependent on the detecting wavelength. In general, the fluorescence decay is fast at the shorter wavelengths while slower at longer wavelengths. Furthermore, the decay data of longer wavelengths show a clear rise at the beginning but this rise is not detected in the decay at shorter wavelengths. Similar results of several different chromophores have been reported,[24−30,34−36] and for each chromophore, the reason for this wavelength dependence is different: it may be the result of the vibration relaxation, or the torsion of chemical bonds, or the interplay (coupling) of them, or the solvation dynamics.

In our present work, all of the dimer molecules have similar decay behavior (data not shown in figure) with the monomer, the similar wave dependence and the decay lifetimes are in the same magnitude. This similarity of dynamic behavior, as well as in their steady-state spectra, implies that the dimerization has not brought dramatic changes to the deactive processes of the excited state of hemicyanine. That is, the change of electronic structure caused by photoactive process (excitation transition and deactive transition) of those dimer molecules occurs still in "one" chromophore, not in the two chromophores collectively.

The decay curves at each different detecting wavelength can be well fitted by the convolution between the instrumental response function with a multiexponential decay (or rise and decay at longer wavelengths) function, expressed as

$$I(t) = R(t) \otimes \{\sum_i A_i \exp(-t/\tau_i) + \sum_j B_j \exp(-t/\tau_j)\} \quad (1)$$

where the $R(t)$ is the instrumental response function, $\tau_i$ the lifetime of the $i$th component of the decay components and $\tau_j$ the lifetime of the $j$th components of the rise components, $A_i$ and $B_j$ the preexponential factors of each component. The open circles in Figure 5 represent the experimental data (for the sake of clarity, not all of them are shown here) and the solid curves are the fitting results. The results of curve fitting are listed as Table 1.

The change of the curve fitting at different detecting wavelength is quite regular. When the detecting wavelength is at the blue edge of the fluorescence band, the decay can be fitted well by a two-exponential decay function; while with the increase of the detecting wavelength, a rise component is introduced into the fitting function, and then the decay curve can be well fitted by the sum of one-exponential rise with either two-exponential or three-exponential decay. When the detecting wavelength is located at the far-red edge of the fluorescence band, the rise part of the decay curve is very clear and in this case one more rise component may be added to better fit the data of the rise part; and the decay part can be well fitted via a one-exponential decay function.

The fitting results of the decay part, that is, the values of the decay lifetime, can be roughly divided into two major components: one is fast and the other is relatively slow. The fast one is from several hundred femtosecond to several picosecond and the slower one is from several picosecond to several tens of picosecond. At several wavelengths, the fast one may be "split" into two "sub-components" to fit the data better, although this splitting might not represent the real deactive process. With the increase of the detecting wavelength, the values of each component, the fast one and the slow one, are gradually increased. The fast one disappears at the several longest detecting wavelengths, whereas the slower component tends to be a constant value at the longest detecting wavelengths. The gradually increased lifetime indicates that the evolution of the excited state may be a barrierless progress, and the constant value of decay lifetime at the long wavelengths implies the probable existence of a nonradiative "sink" region on the potential energy surface of excited state. This situation is quite similar to the case described by BFO theory[37,38] and to the theoretical calculations interpreting the ultrafast decay behavior of the polymethine cyanines.[27] The very fast decay observed in the blue wing of the fluorescence band can be considered as a motion of the excited-state wave packet out of the Franck−Condon region, and the constant lifetime value of the long wavelengths can be regarded as the rate of the nonradiative transition from excited state to ground state.

The deactive processes of the excited state of hemicyanine have been studied for several decades and one of the important features of the excited state is the formation of twisting intramolecular charge transfer (TICT) state.[39] TICT is considered as a nonradiative but favorable state for the excited state of hemicyanine, especially in polar solvent. The TICT formation is responsible for the low fluorescence quantum yield (<1%) of hemicyanine in methanol. Thus, in our system, there are at least 4 major processes that should be taken into account for the ultrafast decay behavior: (a) the vibrational relaxation from higher vibrational states to lower ones; (b) the formation of TICT, that is, the twisting (torsion) motion of the chromophore; (c) the solvation dynamics of the solvent; and (d) the transitions (radiative and nonradiative) between the excited state and the ground state.

**TABLE 1: Curve Fitting Parameters of Fluorescence Up-conversion Decays**

| $\lambda$(nm) | $A_1$(%) | $\tau_1$(ps) | $A_2$(%) | $\tau_2$(ps) | $A_3$(%) | $\tau_3$(ps) | $B_4$(%) | $\tau_4$(ps) | $B_5$(%) | $\tau_5$(ps) |
|---|---|---|---|---|---|---|---|---|---|---|
| | | | | | M | | | | | |
| 535 | *91.9* | 0.978 | | | *8.1* | 9.98 | | | | |
| 545 | *90.9* | 0.755 | | | *9.1* | 10.9 | | | | |
| 555 | *87.4* | 1.10 | | | *12.6* | 14.4 | | | | |
| 565 | *63.7* | 0.757 | *26.6* | 3.19 | *9.7* | 23.6 | *−100* | 0.144 | | |
| 575 | *55.0* | 0.829 | *30.4* | 3.22 | *14.6* | 22.9 | *−100* | 0.169 | | |
| 585 | *69.8* | 2.15 | | | *30.2* | 22.9 | *−100* | 0.156 | | |
| 595 | *56.9* | 2.76 | | | *43.1* | 24.1 | *−100* | 0.203 | | |
| 605 | *48.6* | 3.70 | | | *51.4* | 28.6 | *−100* | 0.243 | | |
| 615 | *36.1* | 3.62 | | | *63.9* | 31.3 | *−100* | 0.375 | | |
| 625 | | | | | *100* | 25.6 | *−100* | 1.45 | | |
| 635 | | | | | *100* | 25.7 | *−53.0* | 3.35 | *−47.0* | *0.579* |
| 645 | | | | | *100* | 26.3 | *−51.9* | 3.46 | *−48.1* | *0.858* |
| | | | | | B3 | | | | | |
| 545 | *89.5* | 0.458 | | | *10.5* | 5.05 | | | | |
| 555 | *89.3* | 0.865 | | | *10.7* | 11.8 | | | | |
| 565 | *83.1* | 0.893 | | | *16.9* | 12.2 | | | | |
| 575 | *60.2* | 0.640 | *28.2* | *3.06* | *11.6* | 22.9 | *−100* | 0.139 | | |
| 585 | *56.3* | 0.900 | *25.0* | *3.80* | *18.7* | 18.8 | *−100* | 0.135 | | |
| 595 | *57.5* | 2.55 | | | *42.5* | 23.6 | *−100* | 0.133 | | |
| 605 | *40.9* | 3.59 | | | *59.1* | 24.5 | *−100* | 0.200 | | |
| 615 | *15.7* | 14.8 | | | *84.3* | 29.8 | *−100* | 0.430 | | |
| 625 | | | | | *100* | 31.9 | *−54.2* | 0.242 | *−45.8* | *1.33* |
| 635 | | | | | *100* | 32.7 | *−47.9* | 0.447 | *−52.1* | *1.92* |
| | | | | | B5 | | | | | |
| 540 | *91.3* | 0.786 | | | *8.7* | 12.9 | | | | |
| 550 | *88.0* | 0.866 | | | *12.0* | 15.3 | | | | |
| 560 | *56.8* | 0.583 | *33.4* | *2.51* | *9.8* | 25.9 | *−100* | 0.120 | | |
| 570 | *51.5* | 0.689 | *31.8* | *3.01* | *16.7* | 27.2 | *−100* | 0.186 | | |
| 580 | *64.1* | 2.30 | | | *35.9* | 26.5 | *−100* | 0.145 | | |
| 590 | *50.0* | 2.93 | | | *50.0* | 28.6 | *−100* | 0.195 | | |
| 600 | *30.8* | 3.86 | | | *69.2* | 29.9 | *−100* | 0.258 | | |
| 610 | *30.5* | 1.53 | | | *69.5* | 29.5 | *−100* | 0.529 | | |
| 620 | | | | | *100* | 29.7 | *−100* | 0.420 | | |
| 630 | | | | | *100* | 30.5 | *−69.0* | 0.383 | *−31.0* | *2.59* |
| 640 | | | | | *100* | 32.9 | *−61.0* | 0.206 | *−39.0* | *2.76* |
| | | | | | B12 | | | | | |
| 530 | *86.1* | 0.677 | | | *13.9* | 5.80 | | | | |
| 540 | *84.5* | 0.750 | | | *15.5* | 7.68 | | | | |
| 550 | *82.0* | 1.48 | | | *18.0* | 21.7 | | | | |
| 560 | *50.8* | 0.887 | *32.0* | *3.64* | *17.2* | 27.9 | *−100* | 0.173 | | |
| 570 | *56.4* | 1.38 | *25.3* | *5.90* | *18.3* | 35.3 | *−100* | 0.228 | | |
| 580 | *52.8* | 3.69 | | | *47.2* | 32.3 | *−100* | 0.190 | | |
| 595 | *35.5* | 5.93 | | | *64.5* | 33.6 | *−100* | 0.294 | | |
| 600 | *38.4* | 6.53 | | | *61.6* | 37.4 | *−100* | 0.284 | | |
| 610 | | | | | *100* | 35.8 | *−100* | 0.543 | | |
| 620 | | | | | *100* | 38.5 | *−100* | 0.645 | | |
| 630 | | | | | *100* | 40.7 | *−100* | 1.09 | | |
| 640 | | | | | *100* | 42.3 | *−100* | 1.59 | | |

**3.3. Transient Fluorescence Spectra Reconstruction and Time Dependent Stokes Shift.** The apparent existence of the rise component of the fluorescence decay at long wavelengths of these four dyes reveals the red shift of the fluorescence emission. Usually, this phenomenon is called "time dependent Stokes shift", a powerful method to investigate the solvation dynamics of solvent. This dynamic Stokes shift is typically represented by a correlation function[24]

$$C_\nu(t) = \frac{\nu(t) - \nu(\infty)}{\nu(0) - \nu(\infty)} \qquad (2)$$

where $\nu(0)$ and $\nu(\infty)$ are the frequencies of the peak of the transient emission spectrum immediately after the pumping laser excitation and when equilibrium has been achieved, respectively. $\nu(t)$ is the peak frequency of the transient emission got at different time.

Usually, a correct correlation function for a certain solvent is obtained by measuring the solvation response of the fluorescence of a probe molecule, whose emission is only affected by the energetics of the interaction between solute and solvent molecules, i.e., the other relaxation process should be weak enough to be ignored. Evidently, our system does not meet this criterion. However, by comparing with the results of the perfect probe molecules, the other effects on the relaxation, such as vibrational relaxation and TICT formation, might be observed.

To acquire the peak positions of the transient emission spectra at different moments, the spectral reconstruction method of Meroncelli and Fleming[29,40] is applied. The steps of this method are as follows: (i) The fluorescence up-conversion decay curves are fitted by eq 1, which is the convolution of the instrumental response function with the real decay function. (ii) For each detection wavelength, the time-integrated fluorescence decay transient, which is deconvoluted from the experimental data with the instrumental response function by the previous step, is normalized to the intensity of the calibrated steady-state fluorescence spectrum at the corresponding wavelength. This

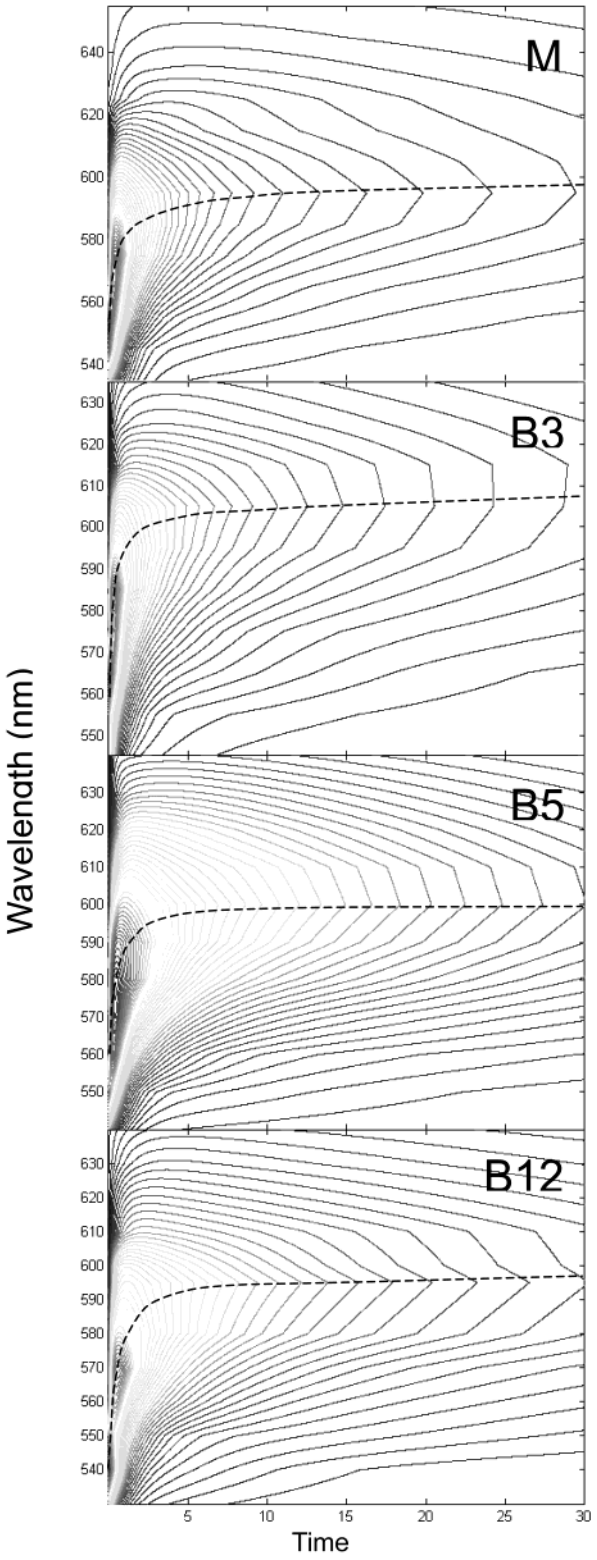


**Figure 6.** Reconstructed fluorescence transient. The dashed lines represent the time dependent fluorescence emission peaks.

step of the procedure is adopted to avoid the wavelength-dependent instrumental responsibility (collecting efficiency of fluorescence, different SFG efficiency, and the sensitivity of detector, etc.). (iii) The fluorescence intensity at time $t$ in the normalized deconvoluted transients at each detection wavelength is picked out and plotted versus the wavelength to construct the transient fluorescence spectrum at time $t$. Figure 6 shows the result of this step of the four dyes by the style of contour

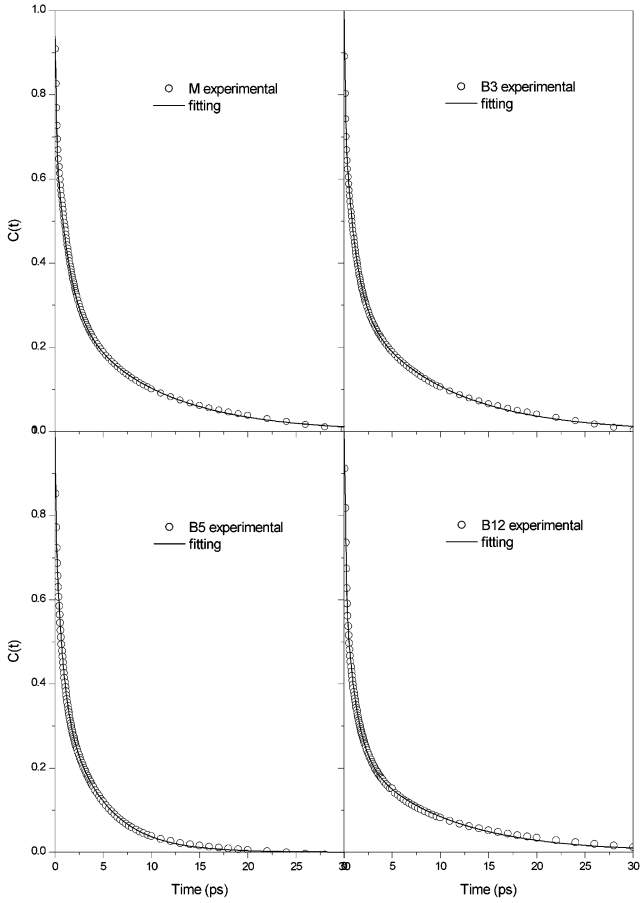


**Figure 7.** Time dependent Stokes shift function and the fitting results. The open circles are experimental results and the solid lines are fitting results by using eq 3.

plots of fluorescence intensity with wavelength and decay time as the coordinates. (iv) The transient spectra at different time are transposed to a wavenumber scale and fitted with a log-normal shape function. Thus, the peak position of each time-resolved spectrum can be obtained from the fitting curves.

The relationship between the peak of fluorescence transient and the decay time is exactly the spectral response function. The data acquired from the spectral reconstruction procedure have been plotted in Figure 7 as open circles. The fitting function of this time-dependent Stokes shift function (TDSSF) is quite different for different solvent molecules, and the dynamic behavior during the initial picosecond of the solvation process is essential. For the small high polar solvent molecules such as water and methanol, a function (eq 3)[28,29] which consists of one inertial Gaussian component and a tail containing two exponential decays, has been well applied to describe the TDSSF

$$C_\nu(t) \propto A_g \exp\left(-\frac{1}{2}t^2\omega_g^2\right) + A_1 \exp(-t/\tau_1) + A_2 \exp(-t/\tau_2) \quad (3)$$

where the ultrafast Gaussian component, whose typical value is 50−500 fs, is usually considered as the ballistic motion of the solvent molecules in the modified field of the solute;[41] it can also be described as the "inertial free streaming" motions of solvent molecules,[29] which are collisionless rotational motions within the solvent cage. The results of deuterium isotope effect on the solvation dynamics of a dye molecule in methanol reported by Joo et al.[42] show that the ultrafast component may be originated from the collective dispersive solvent motion.

**TABLE 2: Solvation Dynamics Function Paremeters**

| solute | $A_g$(%) | $\omega_g$($ps^{-1}$) | $A_1$(%) | $\tau_1$(ps) | $A_2$(%) | $\tau_2$(ps) |
|---|---|---|---|---|---|---|
| M | 21.9 | 7.8 | 41.1 | 1.3 | 31.0 | 9.1 |
| B3 | 22.5 | 8.5 | 45.8 | 1.1 | 31.7 | 9.3 |
| B5 | 15.4 | 12 | 44.8 | 0.67 | 39.8 | 4.2 |
| B12 | 31.6 | 6.3 | 43.2 | 1.1 | 25.2 | 9.2 |
| DCM[a] | 20 | 6 | 50 | 0.7 | 30 | 5 |

[a] Data measured by Glasbeek et al.[29]

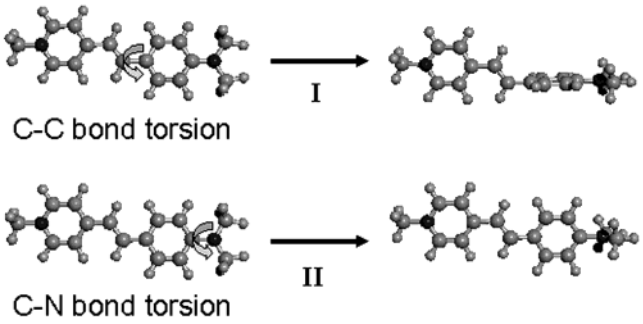


**Figure 8.** Schematic illustration for the two pathways to form the TICT state.

Evidently, this ultrafast component is closely related to the structure of solvent cage, i.e., the closest several layers of solvent molecules. The exponential components are due to the diffusive (rotational diffusion) motions of the solvent molecules.[29]

The fitting results are listed in Table 2. The fitting parameters of DCM, which are cited from Glasbeek et al.,[29] are also listed in the table for comparison. Among these four dyes in our work, B5 is in unique contrast with the other three, which have similar values of each component. To give a more detailed account, all three values of decay lifetime of B5, one Gaussian and two exponential, are shorter than those of M, B3, and B12. B5 has similar lifetime values of exponential components as those of DCM, whereas the other three have much longer values. On the contrary, the lifetime value of Gaussian component of B5 (~80 fs) is much shorter than that of DCM, whereas the other three have similar values as those of DCM (~160 fs). In general, the difference of Gaussian component between B5 and other dyes (including DCM) indicates that there should be difference between the solvent cages of B5 and the others. Furthermore, the difference of exponential components between the M, B3, B12 and DCM implies that some other process should exist beyond the normal solvation response of solvent diffusion and also contribute to the Stokes shift, whereas in B5 this process may not occur. It should be pointed out that although this model, in which the solvation process in our system can be expressed as a Gaussian component with two exponential decays, might not be exclusive, it is self-consistent in our system.

**3.4. TICT Formation and the Potential Energy Surface.** TICT is a dominant reaction path for the evolution of excited state of hemicyanine. The partial charge will transfer from the pyridium moiety of chromophore to the aniline moiety during the intramolecular twisting of the excited state of hemicyanine. Although the concept of TICT originated from the dual fluorescence observation,[43−46] the TICT state of hemicyanine is considered to be a nonradiative state, and the formation is barrierless in polar solvent.[39,47−50] There has been no consensus concerning the torsion mode of TICT formation of hemicyanine but the most recent published works tend to believe that the twisting takes place around the aniline ring through C−C single bond (Figure 8, path I) but not around the dimethyl group through C−N bond (path II). Our semiempirical quantum calculations (AM1) also support this point of view: Figure 9 is

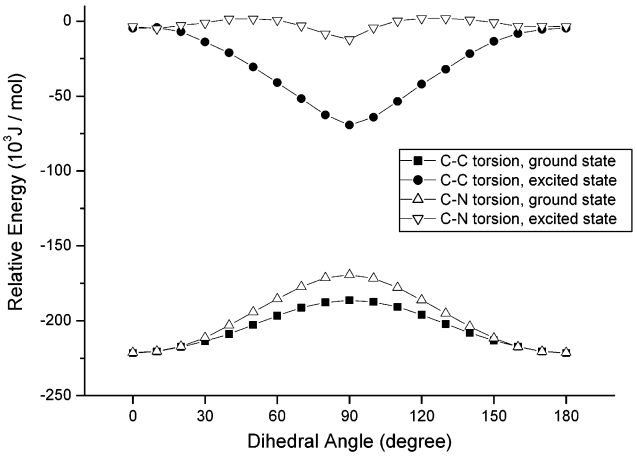


**Figure 9.** Calculation results of the torsion potential energy surface of different twisting modes. The solid symbols represent the results of twisting the aniline ring; the open symbols represent the results of twisting the dimethylamine group.

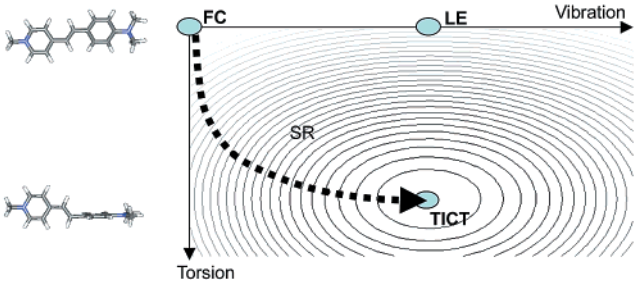


**Figure 10.** Structural relaxation pathway of excited state. FC: Franck−Condon state; LE: Local excited state; TICT: twisted intramolecular charge transfer state; SR: structural relaxation pathway.

the calculation results of the potential energy of the $S_1$ and $S_0$ states of hemicyanine, with different torsion degrees around the two bonds described above. Although our calculations have not taken the solvent into account, at least on the qualitative level, it is clear that the torsion around the C−C bond benefits the formation of TICT state a great deal.

Now turn to the situation in which the motions of the wave packet (of the population of state) when the hemicyanine chromophore is excited to a high vibrational level of the first singlet excited state under our experimental conditions. First, let us not take into account the solvent dynamics and the transition between the excited state and the ground state; hence, there will be two major deactive processes, as shown in Figure 10, of the excited-state wave packet within the S1 state: vibrational (the stretching) and torsional (the twisting) relaxations. According to the theoretical results of Robb et al.,[27] as well as Gong's experimental results[30] with the same experimental setup of this work, our situation is quite similar to the case of short-length polymethine cyanine. Their calculations show that in this case the stretching modes strongly couple with the torsion mode and the relaxation from the Franck−Condon (FC) region to the equilibrium twisting state is in a time scale of several picoseconds. In our work, the real situation is more complex than the simplified case for calculation: the solvation dynamics cannot be ignored and the two-state (excited state and ground state) two-mode (stretching and twisting) model is no longer suitable. Figure 11 is a schematic illustration of the potential energy surfaces of both the excited state and the ground state. It can be summarized as a "two-state three-mode" model, the additional mode being the solvation dynamics. In the figure, these three coupled modes are assigned to two parts: solvation

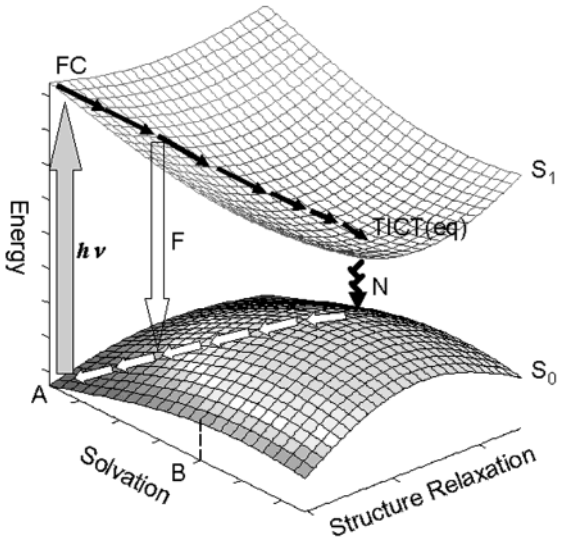


**Figure 11.** Schematic illustration of the potential energy surfaces of both the excited state and the ground state. F: fluorescence transition; N: nonradiative transition; TICT(eq): the equilibrium TICT state with salvation (B represents the most stable coordinate point of excited state by salvation process).

and structure relaxation; the latter is the reaction path described in Figure 10, and it is combined with the stretching and twisting motions, which can be considered as the two coordinates for the three-dimensional potential energy surface plots, as shown in Figure 11. The excited state wave packet is initially located in FC region, then moves through the potential energy surface toward the TICT region, which is a sink-like state and the nonradiative transition takes place there. With the evolution of the excited state, the fluorescence emission red-shifts and the rise time appears at longer wavelengths. The multiexponential decay is due to the nonexclusive deactive paths of the wave packet: (a) the friction within the S1 state, i.e., the "friction" on the surface; and (b) the nonradiative transition between the states. Finally, the wave packet stays around the TICT state, and as we have discussed, that the fitting results of those decay curves at longer wavelengths, the decay lifetime tends to be a constant, which is due to the nonradiative transition from the TICT state to the ground state. Although this "two-state three-mode" model might not be all-inclusive, it is an idealized simple model and viable.

All of that which we have discussed above in this subsection are based on the isolated chromophore of hemicyanine. M is certainly suitable for our assumption. If the TICT state of M is radiative, then M and DCM should be similar to each other in solvation dynamics behavior because the TICT state of DCM is considered as a fluorescent state and its formation is very quick (similar to the situation of C152 molecule[30]). It is the easy formation of nonradiative TICT state that brings out the difference in the exponential decay lifetimes between M and DCM. From the magnitude of difference, it can be estimated that the torsion motion takes place within several picoseconds, which is comparable to the results of other similar twisting motions.

As for the dimer molecules, two of them (B3 and B12) have almost the same behavior as M. This might be explained by the structural factor of the molecules. It has been affirmed by several experiments of ours that it is difficult for the two chromophores in B3 to form a U-shaped folded conformation because the two positive charged pyridium moieties are too close together. Hence, the most possible conformation of B3 is V-shaped, and even under confined conditions such as the LB

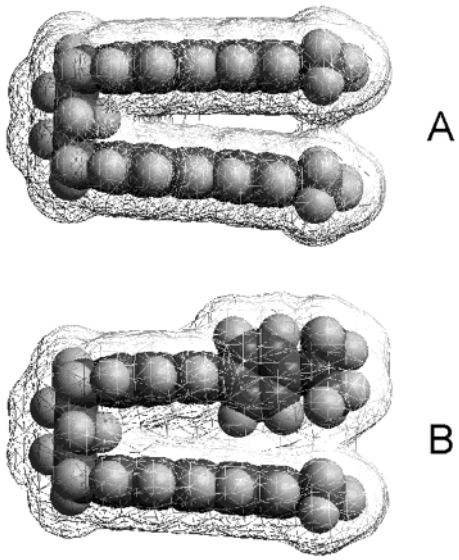


**Figure 12.** Folded conformation (A) of B5 and the corresponding twisting conformation (B). The meshes are the solvent accessible surface by using methanol as solvent molecules (diameter is 0.4 nm).

compressing process, the two chromophores cannot be forced to be parallel. Thus, the two chromophores in B3 are quite well separated from each other. As we have mentioned in the discussion on the steady-state spectra, the linkage of B12 is quite long, so that the two chromophores in B12 are almost isolated. That is, the hemicyanine chromophores in B3 and in B12 are quite similar to an individual chromophore, and this makes the motion of both the chromophore and the solvent molecules around the chromophore free and similar to the case of M. Consequently, the ultrafast dynamics behavior and the TDSSF of B3 and B12 well coincide with those of M.

The similarity of M, B3 and B12 serves as a foil to the uniqueness of B5 in which the lifetime values of both Gaussian component and exponential components are shorter than the other dyes. Although the explanation for the unique photophysical properties of B5 must be very complex, we believe that the molecular conformation plays a most important role in this difference. The crystallography studies of dimers imply that B5 may have a different favorable conformation from other dimers. From the crystal structure of B5, we get from ethanol solution shows a well folded conformation, in which the two chromophores are almost parallel.[22] This is also realized by molecular mechanics conformation search. But how does this folded conformation influence the solvation process of the chromphore? It seems that the solvent cage of B5 is not the same as that of the other dyes, and the TICT formation process of B5 is not observed. We believe that the folded conformation of B5 will introduce a torsional barrier into the rotation around the C−C bond, and then block the fast formation of TICT state. However, what is the difference between the solvent cage of B5 and those of other dyes? And how is the torsional barrier of the chromophore formed? The following analyses, which focus on the solvation cage of the chromophore, will help to answer these questions.

Figure 12A shows the most favorable structure of B5 in a folded shape, the two chromophores are well orientated, and the distance between them (from the centers of chromophores) is about 0.7 nm. This value is too long for the exciton coupling interaction, as we have proved by the spectroscopic method discussed above, whereas it is short enough to affect the solvation behavior and chromophore motion. The meshes in Figure 12 are the solvent accessible surface (center of solvent

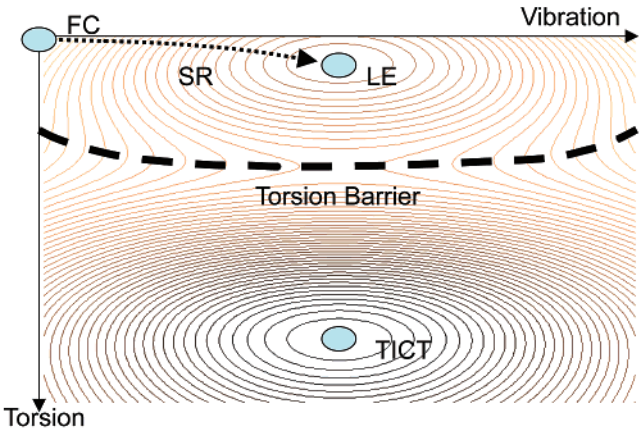


**Figure 13.** Structural relaxation pathway of excited state of B5. FC: Franck−Condon state; LE: Local excited state; TICT: twisted intramolecular charge transfer state; SR: structural relaxation pathway. The bolded dashed line is the position of torsion barrier.

molecules) of B5 when methanol is used as the solvent (set the mean diameter of the methanol molecule at 0.4 nm).[51] Apparently, the folded conformation of B5 makes the access of solvent molecules to the chromophore not so easy as M and the other dimers, in which the chromophores are well isolated. The space between the two nearly parallel chromophores is too limited to admit many solvent molecules. The meshes show that merely one "layer" of the methanol molecules can be squeezed between the two chromophores. This means that the "solvent cage" (which normally consists of several "layers" of molecules) of the hemicyanine chromophores in B5 is different from those in other dyes. This difference may be the nature of the distinctness of the ultrafast Gaussian component of B5.

Furthermore, the folded conformation of B5 also leads to the different behaviors of the twisting motion of the chromophore, which may affect the two exponential decay components of TDSSF. The formation of TICT consequentially correlates with the motions of the surrounding solvent molecules. As shown in Figure 12B, with the twisting of one of the chromophores, the solvent accessible surface of each chromophore overlaps each other, indicating that if the parallelity of the chromophores is kept, the TICT formation of the chromophore in B5 will extrude the solvent molecules, which has stayed between the two chromophores in B5, out of the limited space. This will destroy the integrality of the "solvent cage" that has been constructed before; otherwise, the conformation of B5 must be changed to reduce this destruction. Both of these two possibilities will make the formation of TICT state inconvenient, that is, a torsion barrier might be introduced to the excited state potential surface of B5 (Figure 13, in this figure the solvation process is not taken into account). In this case, if the torsion barrier is high enough, the coupling of the vibrational relaxation and the torsion motion will be blocked, and then, the structure relaxation mainly terminates in the LE (local excited) area. Figure 14 is the schematic illustration of the excited state potential energy surface taking the solvation into consideration. To better present the existence of the barrier, in this figure, the torsion motion is made an independent coordinate, whereas the solvation and vibrational relaxation are combined as the other coordinate. The barrier reduces the possibility of torsion, so that the formation of TICT state becomes slower than in normal situation. Consequently, the emissive red-shift caused by the TICT formation is not easily observed in B5 in the initial period (30 ps), and the solvation behavior of B5 should be similar to that of DCM but not to that of M, B3 or B12. Although the

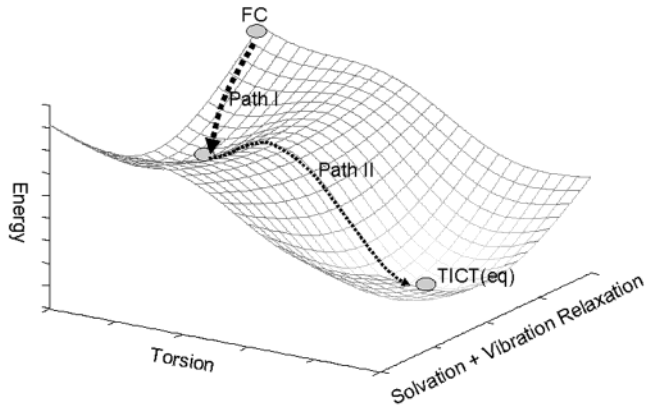


**Figure 14.** Schematic illustration of the potential energy surface of the excited state of B5. TICT(eq): the equilibrium TICT state with salvation; Path I is barrierless and Path II is barrier-crossing process.

accurate value of the barrier height cannot be easily acquired from our experiments or theoretical calculations, we can estimate that this barrier should not be very high. First, it is commonsensical to see that this conformation change is not a difficult motion for a molecule in the solution condition. Second, the similar low quantum yields (∼0.1%) of all of the the four dyes indicate that the TICT formation has not been thoroughly blocked so that the barrier-cross is not difficult; otherwise, there should be much stronger fluorescence emission of B5 than of others. Furthermore, the similar values of decay lifetime at longer wavelengths of the dyes indicate that the transitions come from the states with similar electronic structures, i.e., all of them should belong to the "sink" region (of TICT state) and the existence of barrier does not affect the nonradiative transition between $S_1$ and the ground state. The gradually changed fitting parameters of decays also indicate a "barrierless" potential energy surface of B5. All of these indicate that the evolution of the excited state of B5 is through a path which is plotted in Figure 14 as path I, with which the evolution is barrierless. The barrier cross (path II) produces a slow formation of TICT state so that the red-shift of fluorescence arisen by TICT formation is much slower than normal and not distinct in the initial period. Consequently, the TDSSF we have observed within 30 ps are mainly due to the solvation and vibrational relaxation, which is similar to the case of DCM[29] and even of Coumarin chromophore.[30]

Another feature of dyes, which can be predicted from our assumption above, is that the total change of the Stokes shift within the initial 30 ps of B5 is less than other three samples because the evolution of the excited state of B5 has not reached the TICT state in this short duration. This corresponds with what we have observed in our TDSSF curve fitting. The amounts of Stokes-shift-changing in the initial 30 ps of the four dyes we have studied here are as follows: M (55 nm), B3 (50 nm), B5 (40 nm) and B12 (56 nm).

## 4. Summary

The ultrafast fluorescence up-conversion method has been employed to investigate a series of hemicyanine dyes in methanol. These dyes are one monomer and three dimers with different lengths of linkage joining the two chromophores. There are no distinct differences between their steady state spectra, indicating the similar nature of transition between the ground states and the excited states of these dyes. The multiexponential fitting results of the ultrafast fluorescence up-conversion decays reveal a similar tendency of the four dyes; they can be fitted as

two or more exponential decays at shorter wavelengths (blue edge of the emission band), and the sum of exponential rise(s) and decay(s) at longer wavelengths (red edge of the emission band). The nearly constant values of the decay lifetime at longer wavelengths and the gradually changed parameters of fitting indicate that there might be a nonradiative "sink" region at the potential energy surface of excited state and that the evolution path of the excited state is barrierless. The time dependent Stokes shift (TDSS) function fitting shows the difference between B5 and the other three dyes, which is probably due to the conformation difference of these dyes. The formation of TICT state in hemicyanine chromophore also contributes to the time dependent fluorescence red-shift during the initial period after the excitation. This is how a "two-state (ground state and excited state) three-mode (vibrational relaxation, torsion, and solvation)" model is applied to our system. To explain the unique TDSS behavior of B5, we propose that the difficult TICT formation of B5 caused by the folded conformation changes the potential energy surface of excited state. This proposition agrees with our experimental results in B5, in which the TDSS contributed by the TICT formation is hardly observed and the total amount of fluorescence shift is less than the other dyes in the initial 30 ps.

**Acknowledgment.** This work is supported by the State Key Program of Fundamental Research (Grant Nos. G1998061308 and 2001CCD04300), the National Natural Science Foundation of China (Grant Nos. 20023005 and 59872001) and the Doctoral Program of Higher Education (99000132). Prof. Yuxiang Weng and Prof. Hongfei Wang are also gratefully acknowledged by Y. H. for their kind help.

## References and Notes

(1) Abraham, U. *An Introduction to Ultrathin Organic Films: From Langmuir−Blodgett to Self-Assembly*; Academic Press: Boston, 1991.
(2) Zhao, C. F.; Gvishi, R.; Narang, U.; Ruland, G.; Prasad, P. N. *J. Phys. Chem.* **1996**, *100*, 4526.
(3) For example, see: Jones, M. A.; Bohn, P. W. *Anal. Chem.* **2000**, *72*, 3776. and references therein.
(4) Ephardt, H.; Fromherz, P. *J. Phys. Chem.* **1989**, *93*, 7717.
(5) For expample, see Duan, X. M.; Konami, H.; Okada, S.; Oikawa, H.; Matsuda, H.; Nakanishi, H. *J. Phys. Chem.* **1996**, *100*, 17 780. and references therein.
(6) Ashwell, G. J.; Jackson, P. D.; Crossland, W. A. *Nature* **1994**, *368*, 438.
(7) Ashwell, G. J.; Jackson, P. D.; Lochun, D.; Thompson, P. A.; Crossland, W. A.; Bahra, G. S.; Brown, C. R.; Jasper, C. *Proc. R. Soc. London A* **1994**, *445*, 385.
(8) Lang, A. D.; Zhai, J.; Huang, C. H.; Gan, L. B.; Zhao, Y. L.; Zhou, D. J.; Chen, Z. D. *J. Phys. Chem. B* **1998**, *102*, 1424.
(9) Wang, Z. S.; Li, F. Y.; Huang, C. H.; Wang, L.; Wei, M.; Jin, L. P.; Li, N. Q. *J. Phys. Chem. B* **2000**, *104*, 9676.
(10) Li, F.; Zheng, J.; Huang, C.; Jin, L.; Zhuang, J.; Guo, J.; Zhao, X.; Liu, T. *J. Phys. Chem. B* **2000**, *104*, 5090.
(11) Wu, D. G.; Huang, C. H.; Gan, L. B.; Zhang, W.; Zheng, J.; Luo, H. X.; Li, N. Q. *J. Phys. Chem. B* **1999**, *103*, 4377.
(12) Wu, D. G.; Huang, C. H.; Huang, Y.; Gan, L. B.; Yu, A. C.; Ying, L. M.; Zhao, X. S. *J. Phys. Chem. B* **1999**, *103*, 7130.
(13) me-dimer
(14) Mishra, J. K.; Behera, P. K.; Parida, S. K.; Mishra, B. K. *Ind. J. Chem.* **1992**, *31B*, 118.
(15) Chibisov, A. K.; Zakharova, G. V.; Gorner, H.; Sogulyaev, Y. A.; Mushkalo, I. L.; Tolmachev, A. I. *J. Phys. Chem.* **1995**, *99*, 886.
(16) Mishra, B. K.; Kuanar, M.; Mishra, A.; Behera, G. B. *Bull. Chem. Soc. Jpn.* **1996**, *69*, 2581.
(17) Bazan, G. C.; Oldham, W. J.; Lachicotte, R. J.; Tretiak, S.; Chernyak, V.; Mukamel, S. *J. Am. Chem. Soc.* **1998**, *120*, 9188.
(18) Song, X.; Perlstein, J.; Whitten, D. G. *J. Phys. Chem. A* **1998**, *102*, 5440.
(19) Lu, L.; Lachicotte, R. J.; Penner, T. L.; Peristein, J.; Whitter, D. G. *J. Am. Chem. Soc.* **1999**, *121*, 8146.
(20) Zeena, S.; Thomas, K. G. *J. Am. Chem. Soc.* **2001**, *123*, 7859.
(21) Bartholomew, G. P.; Bazan, G. C. *Acc. Chem. Res.* **2001**, *34*, 30.
(22) Huang, Y.; Cheng, T.; Li, F.; Huang, C.-H.; Hou, T.; Yu, A.; Zhao, X.; Xu, X. *J. Phys. Chem. B* **2002**, *106*, 10020.
(23) Huang, Y.; Cheng, T.; Li, F.; Huang, C.-H.; Cai, Z.; Zeng, X.; Zhou, J. *J. Phys. Chem. B* **2002**, *106*, 10031.
(24) For example, see Kovalenko, S. A.; Eilers-Konig, N.; Senyushkina, T. A.; Ernsting, N. P. *J. Phys. Chem. A* **2001**, *105*, 4834, and references therein.
(25) Rossky, P. J.; Simon, J. D. *Nature* **1994**, *370*, 263.
(26) Walker, G. C.; Akesson, E.; Johnson, A. E.; Levinger, N. E.; Barbara, P. F. *J. Phys. Chem.* **1992**, *96*, 3728.
(27) Sanchez-Galvez, A.; Hunt, P.; Robb, M. A.; Olivucci, M.; Vreven, T.; Schlegel, H. B. *J. Am. Chem. Soc.* **2000**, *122*, 2911.
(28) Jimenez, R.; Fleming, G. R.; Kumar, P. V.; Maroncelli, M. *Nature*, **1994**, *369*, 471.
(29) van der Meulen, P.; Zhang, H.; Jonkman, A. M.; Glasbeek, M. *J. Phys. Chem.* **1996**, *100*, 5367.
(30) Zhang, T.; Chen, C.; Gong, Q.; Yan, W.; Wang, S.; Yang, H.; Jian, H.; Xu, G. *Chem. Phys. Lett.* **1998**, *298*, 236.
(31) Ando, K. *J. Chem. Phys.* **2001**, *114*, 9040.
(32) Gumy, J.-C.; Nicolet, O.; Vauthey, E. *J. Phys. Chem. A* **1999**, *103*, 10 737.
(33) For example, see Evans, C. E.; Song, Q.; Bohn, P. W. *J. Phys. Chem.* **1993**, *97*, 12 302.
(34) Mokhtari, A.; Chesnoy, J.; Laubereau, A. *Chem. Phys. Lett.* **1989**, *155*, 593.
(35) van der Meer, M. J.; Zhang, H.; Rettig, W.; Glasbeek, M. *Chem. Phys. Lett.* **2000**, *320*, 673.
(36) Jurczok, M.; Gustavsson, T.; Mialocq, J.-C.; Rettig, W. *Chem. Phys. Lett.* **2001**, *344*, 357.
(37) Bagchi, B.; Fleming, G. R.; Oxtoby, D. W. *J. Chem. Phys.* **1983**, *78*, 7375.
(38) Changenet, P.; Zhang, H.; van der Meer, M. J.; Glasbeek, M.; Plaza, P.; Martin, M. M. *J. Phys. Chem. A* **1998**, *102*, 6716.
(39) Kim, J.; Lee, M. *J. Phys. Chem. A* **1999**, *103*, 3378, and references therein.
(40) Maroncelli, M.; Fleming, G. R. *J. Chem. Phys.* **1987**, *86*, 6221.
(41) Brown, R.; Middelhoek, R.; Glasbeek, M. *J. Chem. Phys.* **1999**, *111*, 3616.
(42) Lee, S.-H.; Lee, J.-H.; Joo, T. *J. Chem. Phys.* **1999**, *110*, 10 969.
(43) Herbich, J.; Grabowski, Z. R.; Wojtowicz, H.; Golankiewicz, K. *J. Phys. Chem.* **1989**, *93*, 3439.
(44) Grabowski, Z. R. *Pure Appl. Chem.* **1992**, *64*, 1249.
(45) Maus, M.; Rettig, W.; Bonafoux, D.; Lapouyade, R. *J. Phys. Chem.* **1999**, *103*, 3388.
(46) Bhattacharyya, K.; Chowdhury M. *Chem. Rev.* **1993**, *93*, 507.
(47) Rettig, W. *Top. Curr. Chem.* **1994**, *169*, 253.
(48) Cao, X.; Tolbert, R. W.; McHale, J. L.; Edwards, W. D. *J. Phys. Chem. A* **1998**, *102*, 2739.
(49) Cao, X.; McHale, J. L. *J. Chem. Phys.* **1998**, *109*, 1901.
(50) McHale, J. L. *Acc. Chem. Res.* **2001**, *34*, 265.
(51) Bagchi, B.; Gayathri, *Adv. Chem. Phys.* **1999**, *107*, 1.